ACADEMIC PRESS

Available online at www.sciencedirect.com

SCIENCE DIRECT®

Journal of Sound and Vibration 264 (2003) 411–431

JOURNAL OF SOUND AND VIBRATION

www.elsevier.com/locate/jsvi

The quantification of structure-borne transmission paths by inverse methods. Part 1: Improved singular value rejection methods

A.N. Thite, D.J. Thompson*

Institute of Sound and Vibration Research, University of Southampton, Highfield, Southampton SO17 1BJ, UK

Received 28 August 2001; accepted 20 June 2002

Abstract

Structure-borne sound from installed machinery is often transmitted into a receiver structure via many connection points and several co-ordinate directions at each of them. In order to quantify the contributions from the various connection points, the operational forces at the interfaces, or an equivalent set of forces at some other locations, should be determined. These forces may be combined with measured transfer functions to determine their contributions to the sound at the receiver locations. Inverse methods are becoming widely used, in which a matrix of measured accelerances is inverted at each frequency and used with operational acceleration data to find the forces. Due to poor conditioning of this matrix, however, the results can often be unreliable. In this paper, using both simulations and measurements, an assessment is made of the success and failure of various strategies for dealing with the problems of ill conditioning, in particular over-determination and singular value rejection. In each case the test structure is a rectangular plate, and a wide frequency range is covered to include regions of both low and high modal overlap. Critical for the rejection of singular values is a suitable threshold. It is established that previously used thresholds, based on estimates of error in either accelerances or operational responses, cannot be used universally. An alternative approach is developed in which the accelerance matrix is perturbed by a different amount for each sample of the operational responses. Based on this approach a more robust strategy is proposed which takes account simultaneously of the effect of errors in both the accelerances and operational responses.

*Corresponding author. Tel: +44-23-8059-2510; fax: +44-23-8059-3190.
E-mail address: djt@isvr.soton.ac.uk (D.J. Thompson).

0022-460X/03/$ - see front matter
PII: S0022-460X(02)01202-6

1. Introduction

Structure-borne sound from installed machinery is often transmitted into a receiver structure via many connection points and several co-ordinate directions at each of them. For example, the vibrational energy is transmitted from the engine into the cabin of an automobile through engine mounts and other structural connections, and passes through the structure, to interior panels which radiate into the cabin. In order to quantify the contributions from the various connection points, the operational forces at the interfaces, or an equivalent set of forces at some other locations, should be determined [1–3]. The accuracy with which these forces can be obtained determines the suitability of the application of experimental methods such as transfer path analysis or numerical simulations as tools in understanding the noise problem at hand and ultimately reducing the noise at the receiver location.

The forces causing structure-borne noise often have to be identified indirectly. This involves the use of responses $\{\hat{\mathbf{a}}\}$ measured at a series of locations due to the operational source, in combination with frequency response functions (FRFs) and/or mechano-acoustic transfer functions $[\hat{\mathbf{A}}]$ measured from source locations to these response locations. Since the forces $\mathbf{F}$ satisfy $\{\mathbf{a}\} = [\mathbf{A}]\{\mathbf{F}\}$, or for measured quantities $\{\hat{\mathbf{a}}\} \cong [\hat{\mathbf{A}}]\{\hat{\mathbf{F}}\}$ a matrix of measured FRFs has to be inverted at each frequency. The indirect force identification is, therefore, prone to errors. The forces can contain large errors introduced by the combination of ill conditioning of the FRF matrix at certain frequencies and the errors in the measurement of operational responses and FRFs [4–6].

Over-determining the system can reduce the extreme sensitivity of the inverse method to measurement errors. Since, in the over-determination, the FRF matrix is rectangular, the forces are identified by a least-squared error method. For example, the Moore–Penrose pseudo-inverse can be used $\hat{\mathbf{A}}^{+} = (\hat{\mathbf{A}}^{\mathrm{H}}\hat{\mathbf{A}})^{-1}\hat{\mathbf{A}}^{\mathrm{H}}$, where H indicates the Hermitian transpose. In certain cases however, the over-determination does not help to reduce the magnification of errors [4]. Earlier studies [4–7] have also considered performing a singular value decomposition (SVD) of the FRF matrix $\hat{\mathbf{A}} = \mathbf{U}\mathbf{S}\mathbf{V}^{\mathrm{H}}$ with $\mathbf{U}$ and $\mathbf{V}$ unitary matrices and $\mathbf{S}$ a diagonal matrix containing the singular values s_i. In terms of singular values and unitary matrices the expression for the force vector is given by

$$\{\hat{\mathbf{F}}\} = \mathbf{V}\mathbf{S}^{-1}\mathbf{U}^{\mathrm{H}}\{\hat{\mathbf{a}}\}. \tag{1}$$

The inverse $\mathbf{S}^{-1}$ consists of the diagonal terms $1/s_i$. Small singular values, which can be influenced significantly by measurement noise, thus have a large effect on the inverse. They may therefore usefully be discarded if they are smaller than a threshold value, with $1/s_i$ replaced by 0. This leads to a more reliable estimate of the forces. The problem here is how to estimate the threshold value for the rejection of singular values. In Refs. [4,7] norms of the FRF error matrix or the operational response error vector were adopted with varying degrees of success. As will be seen, however, neither of these is applicable universally.

In this study, simulations and experiments have been carried out on a rectangular steel plate to investigate further the over-determination and singular value rejection strategies. Situations in which the different thresholds fail are demonstrated. In addition the consequences of using different magnitudes of threshold level are discussed. Then a new approach is developed in which the accelerance matrix is resampled for each sample of the operational responses. This is

implemented practically by a perturbation technique. Finally, a combined technique is proposed which results in a robust strategy, which is effective for any combination of response and accelerance errors.

2. Simulations

2.1. Test structure

A simply supported rectangular steel plate of size 600 mm × 500 mm × 1.5 mm was used as a test structure for simulations to represent experiments. Four coherent point forces were applied perpendicular to the plate at randomly selected points. Five locations were chosen for operational response estimates. The arrangement of the plate along with force and acceleration measurement locations is shown in Fig. 1. A further location, marked R, was used as a receiver position.

2.2. Analytical model of the test structure

The accelerance, A, of a simply supported rectangular plate is given by [8]

$$A((x,y),(x_1,y_1)) = \sum_p \sum_q \frac{-\omega^2 \psi_{pq}(x,y)\psi_{pq}(x_1,y_1)}{M_{pq}((\omega_{pq}^2 - \omega^2) + j\mu\omega_{pq}^2)}, \tag{2}$$

where (x,y) is the response location and (x_1,y_1) is the excitation point. p,q are integers, $\psi_{pq} = \sin(p\pi x/a)\sin(q\pi y/b)$ is the mode shape function, $M_{pq} = m_{plate}/4$ is the modal mass where m_{plate} is

Fig. 1. Response (a) and force (F) locations on the plate, (R) is the position of the receiver.

the plate mass. μ is the damping loss factor which is taken here as 0.03 and ω_{pq} is the natural frequency which is given by

$$\omega_{pq} = \left[\left(\frac{p\pi}{a}\right)^2 + \left(\frac{q\pi}{b}\right)^2\right]\sqrt{\frac{D}{\rho h}}, \tag{3}$$

where a and b are the length and width, h is the thickness, ρ is the density, $D = Eh^3/(12(1-v^2))$ is the bending stiffness, E is Young's modulus and v is the Poisson ratio.

The 'exact' FRFs from each forcing location to a series of response locations have been estimated using Eq. (2). The acceleration signals corresponding to 'measured' FRFs were generated using a unit force at each frequency. Both acceleration and force spectra were then corrupted by adding a complex noise signal in the frequency domain. Then, using the usual H_1 estimator [9], the measured FRFs $\hat{\mathbf{A}}$ were determined by averaging over a number of samples, n_{av}.

Using the principle of superposition, the operational responses $\{\hat{\mathbf{a}}\}$ were calculated from the true values of $\mathbf{A}$ and $\mathbf{F}$ and noise was again added to this response signal in the frequency domain to represent measurement noise. The operational forces used in this calculation were broadband and chosen to have a smooth spectrum, weighted such that they are constant with respect to frequency when converted to a one-third octave band representation. Their values were 27, 19, 10 and 6 N. The use of broadband force spectra is considered for simplicity although it is not expected that results would differ qualitatively if a force signal with harmonic spectrum were used, other than the emphasis of particular frequencies. This is because the solution is obtained at each frequency separately. The frequency range used for the study was from 10 Hz to 3.6 kHz. The first resonance is at 25 Hz and there are 200 modes up to 3.6 kHz. The modal overlap, $\mu\omega n$, where n is the modal density, is greater than 1 for frequencies above 600 Hz. The plate response is thus dominated at low frequencies by individual modes, at high frequencies by multiple overlapping modes.

2.3. Noise models and their significance

In the simulations, 'measurement noise' was added to the acceleration signals based on a Gaussian additive noise model with amplitude proportional to frequency, $N(\omega) = C\omega N_{nd}e^{j2\pi N_{ud}}$ where C is a constant, N_{nd} is a normally distributed random number with mean 0 and standard deviation 1 and N_{ud} is a uniformly distributed random number in the range 0–1. Estimating the FRFs results in very low coherence at high frequency depending on the amplitude, C. Fig. 2a shows one of the response signals used in determining the FRFs. It is shown in the form of a velocity in one-third octave bands for ease of presentation. Also shown is the corresponding noise amplitude. The noise level is observed to be significant compared to the response signal in the high-frequency region. One of the operational responses is shown in Fig. 2b along with the corresponding noise signal. Again the noise level can be seen to be significant in the high-frequency region.

The force signals are corrupted by a Gaussian additive model with an amplitude that is constant with frequency before being used in estimating the FRFs. The standard deviation of the amplitude of the noise used in these simulations is 20% of the actual force.

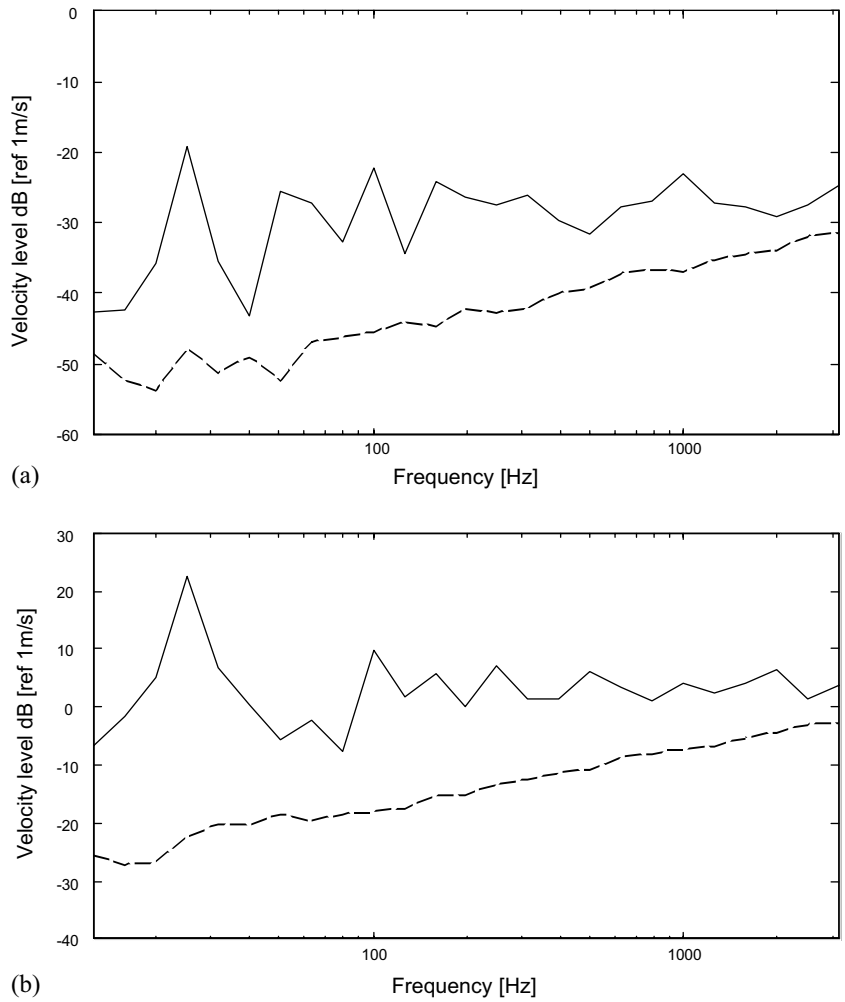

Fig. 2. Comparison of added noise and response signal. ——— , response; — — — noise: (a) noise level in velocity response to estimate FRF and (b) noise level in operational response.

3. Strategies to improve force identification

3.1. Over-determination

As has been pointed out, force identification errors can generally be reduced by over-determination, i.e., using a larger number of responses than the forces to be identified, and employing a least-squared error solution, such as Moore–Penrose pseudo-inversion. This reduction in the error is observed to correspond to an improvement in the condition numbers of the matrix $\hat{\mathbf{A}}$ at some frequencies.

Fig. 3(a) shows the condition number of the (4×4) accelerance matrix using responses a1 to a4. As the number of responses used is increased, many of the peaks in the condition number are

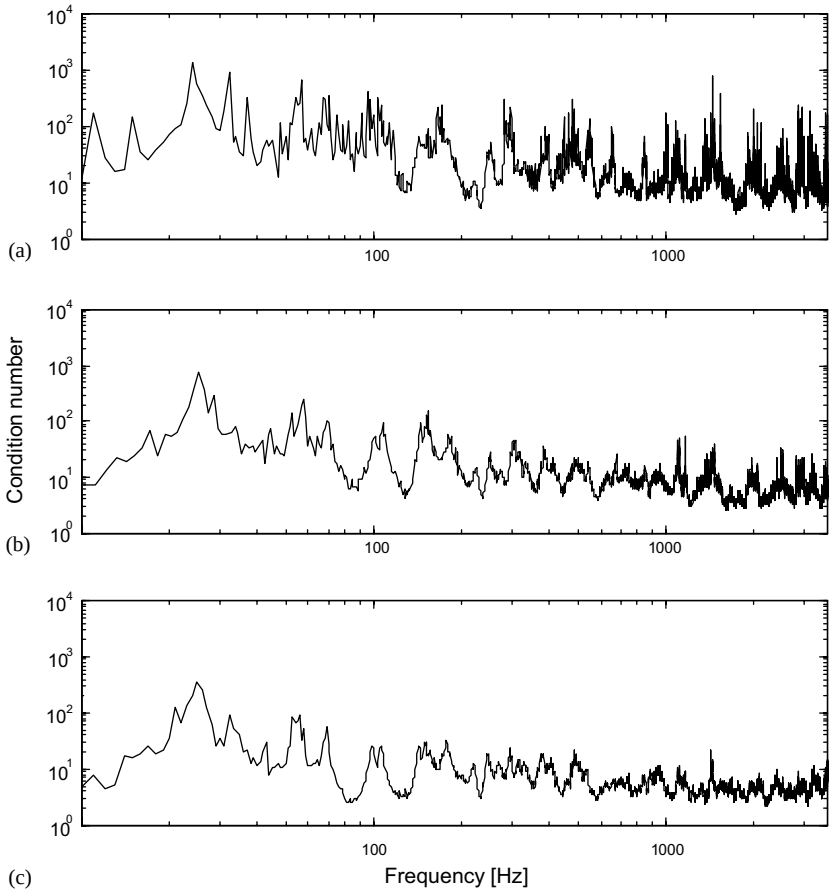

Fig. 3. Condition number of FRF matrix: (a) four sources and four responses; (b) four sources and five responses; and (c) four sources and six responses.

removed as seen in Figs. 3b and c. However, the broad peak at 25 Hz, corresponding to the first mode of the plate, although reduced from over 1000, still reaches 300 for the (6×4) case. The improvement at the next few modes is more significant than at the first mode but peaks remain corresponding to modes at 55, 70, and 100 Hz, etc. This behaviour can be explained as follows. At low frequencies the modal density is very low, so the deflections are dominated by a single mode. These are hence related at all the locations. The placement of forces at any location would excite the same mode and responses at any location would be due to the same mode. This results in dependent columns or rows in the accelerance matrix. Hence, the condition numbers are quite high at these frequencies even if more responses are used. Nevertheless, over-determination reduces the effect of random errors which cause the variation of condition numbers at low frequencies, and at high frequencies the condition numbers of the over-determined system reduce considerably. Here the modal overlap is higher so that many modes contribute to the response at any frequency. This results in lower condition numbers at high frequencies in general for the over-determined case.

The forces identified using a (4×4) FRF matrix are shown in Fig. 4. The forces have been calculated from each of n_s ($n_s = 25$ in all simulations) estimates of operational responses and the mean of these results is shown in the figure. The phase information is also included while taking the average. This method is different to that used previously, e.g., Ref. [4], where forces are calculated directly from the mean of $\{\hat{\mathbf{a}}\}$ and leads to improved results [10]. It should be noted that the calculation is performed in narrow bands (1 Hz spacing) but that the resulting force spectra are converted to one-third octave bands for clarity of presentation. The true force spectra are constant across all one-third octave bands, with the values shown at the right of the figure. Although the actual forces range from 6 to 27 N, the reconstructed forces are all similar in magnitude to one another and mostly between 25 and 100 N. This over-prediction is greatest at low frequencies.

The forces identified for a (5×4) over-determined system by a least-squares solution are shown in Fig. 5. Above 100 Hz the results are better than the square matrix case, especially for the smaller forces. Nevertheless, the forces identified are observed to have large errors in the low-frequency region, as in the square matrix case. This is due to the fact that only a small number of modes contribute significantly to the operational responses in the low-frequency region; this number can be smaller than the number of forces to be identified [11].

Fig. 6 shows the reconstructed response at the 'receiver' position. This is again the mean obtained by averaging n_s predicted responses calculated from the n_s sets of reconstructed forces. Such a method also allows confidence intervals to be determined for the reconstructed response [10]. Even though considerable errors still exist in force identification at low frequencies, the responses predicted are remarkably accurate with over-determination.

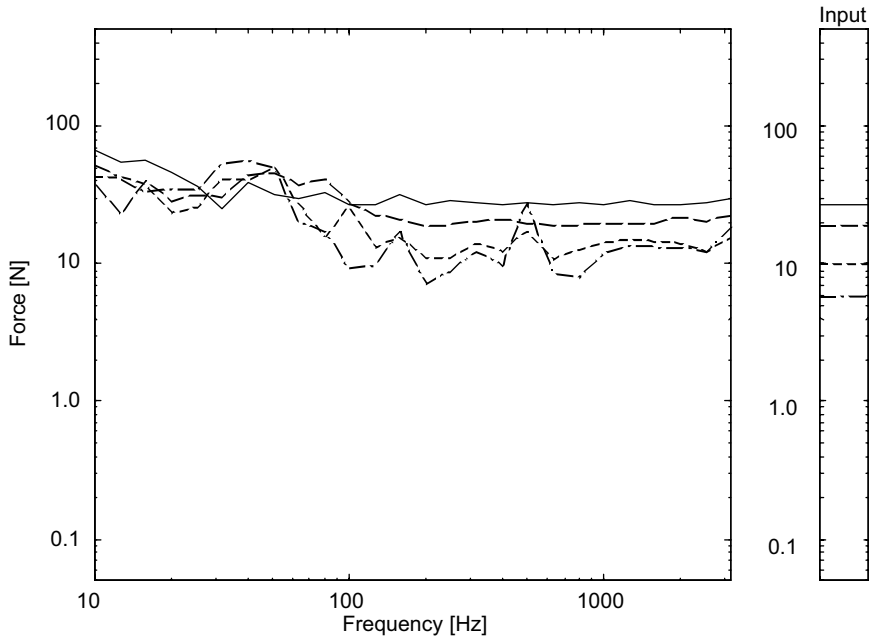

Fig. 4. Reconstructed forces in one-third octave bands for four sources and four responses with all singular values used. ——— , force 1; — — — , force 2; – – – – , force 3; — · — · — , force 4.

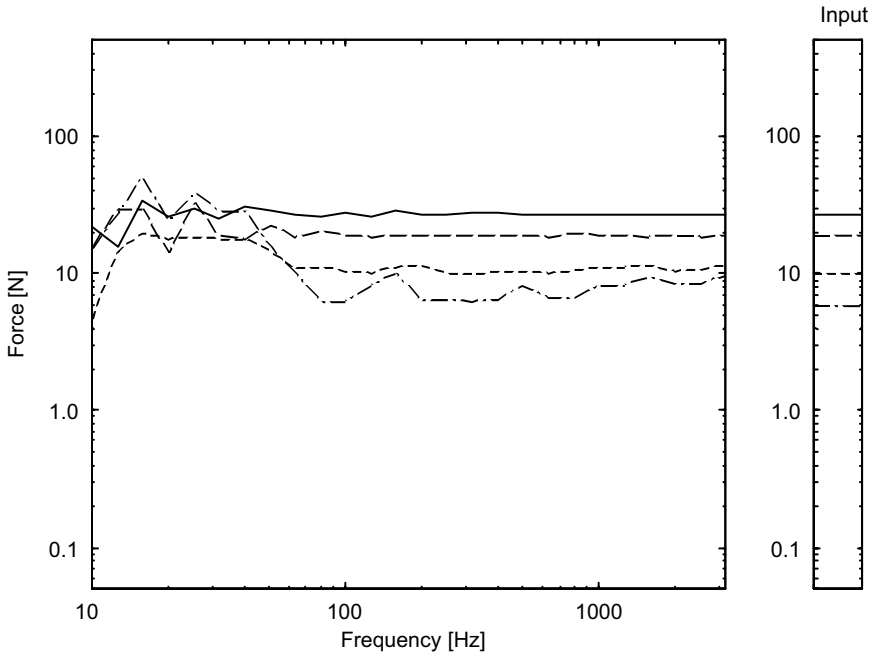

Fig. 5. Reconstructed forces in one-third octave bands for four sources and five responses with all singular values used. ——— , force 1; — — — , force 2; – – – – , force 3; — · — · — , force 4.

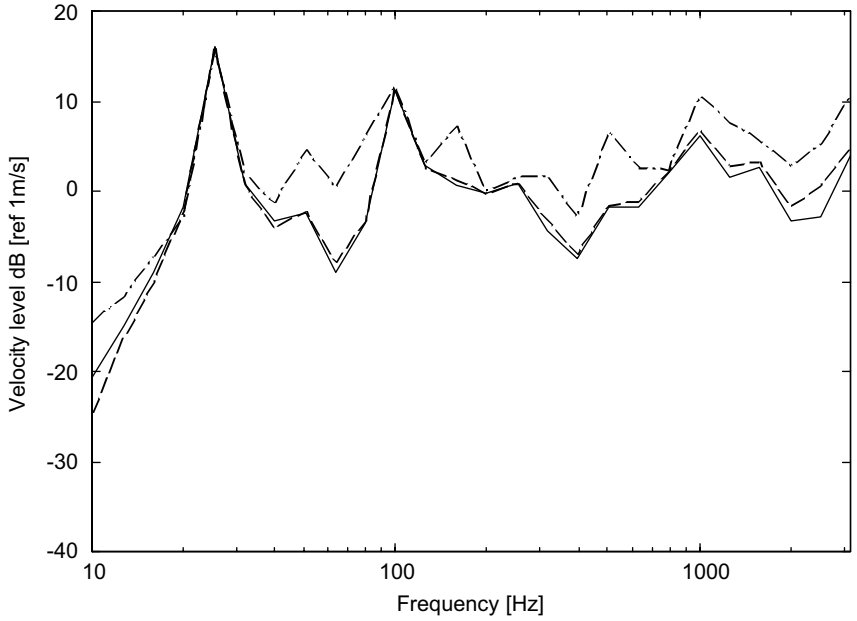

Fig. 6. One-third octave band velocity response with all singular values used. ——— , Actual response; — · — · — , predicted response using 4×4 matrix; — — — , predicted response using 5×4 matrix.

3.2. Singular value rejection

The condition numbers of the FRF matrix can be further improved by discarding small singular values, which are significantly influenced by the measurement noise. For this, the solution has to be written in terms of singular values of the FRF matrix, using SVD as described in Section 1. It may be seen from Eq. (1) that smaller singular values magnify the error in the inversion and also lead to the propagation of errors in the operational responses $\{\hat{\mathbf{a}}\}$. Rejection of these small singular values can help to reduce these errors. The difficulty, however, is to find a suitable threshold for the singular values below which small singular values are rejected. Such a threshold can be determined based on either the error in FRF estimates or the errors in operational responses [4,7]. The singular values rejected depend on the error band used in establishing the threshold. In this section different bandwidths are studied for their effectiveness. The effect of changes in the relative error levels of accelerances and responses is also investigated.

3.2.1. Threshold based on accelerance error

The error in an FRF estimate can be taken as a basis for establishing the singular value rejection threshold. The elements of the FRF error matrix can be constructed following Ref. [9] as

$$E_{ij} = \alpha \left[\frac{(1-\gamma^2_{\omega,ij})}{2n_{av}\gamma^2_{\omega,ij}} \right]^{1/2} |\hat{A}_{\omega,ij}|, \tag{4}$$

where E_{ij} defines an error bound for $\hat{A}_{\omega,ij}$. Here, γ^2 is the coherence and n_{av} is the number of averages used in determining $\hat{\mathbf{A}}$. If α is 1, for instance, E_{ij} represents one standard deviation of $\hat{A}_{ij}$. The norm of the error matrix $\|\mathbf{E}\|_2$ can be used as a threshold to reject the singular values of $[\hat{\mathbf{A}}]$, as suggested in Ref. [4]. If all the singular values are less than the error norm then the largest singular value may be replaced by the error norm itself.

Fig. 7 shows the identified forces in one-third octave band form found by rejecting singular values based on the threshold with $\alpha = 3$, i.e., a band of three standard deviations of the error norm, as used in Ref. [4]. By rejecting singular values based on this threshold, a lot of useful information is discarded during inversion and the identified forces are found to be underestimated at many frequencies. If the error band is reduced to $\pm$ one standard deviation ($\alpha = 1$) the loss of information is restricted. Hence, the forces are identified more reliably, as shown in Fig. 8. This band ($\alpha = 1$) is found to result in a more consistent force identification for any level of accelerance error [10,12].

The predicted responses follow the same trend as the forces as shown in Fig. 9. For the case of the threshold based on $\alpha = 3$, the response is underestimated, whereas for threshold based on $\alpha = 1$ the response prediction is more reliable.

The above criterion can be extended if, instead of comparing individual singular values with the error threshold, the cumulative sum of the last $(n-r)$ singular values is compared with the threshold, with r taking the values $n-1, n-2, \ldots, 1$. This concept is based on the principle that each singular value contributes partially in forming the accelerance matrix as $\mathbf{A}_j = \mathbf{U}_{i,j} s_j \mathbf{V}^{\mathrm{H}}_{j,k}$ for $j,k = 1 \ldots n$ and $i = 1 \ldots m$. When the 2-norm is used in comparing with the threshold, only the largest singular value of the partial accelerance matrix constructed from last $(n-r)$ singular values is compared. This ignores the contribution from the smaller singular values. When

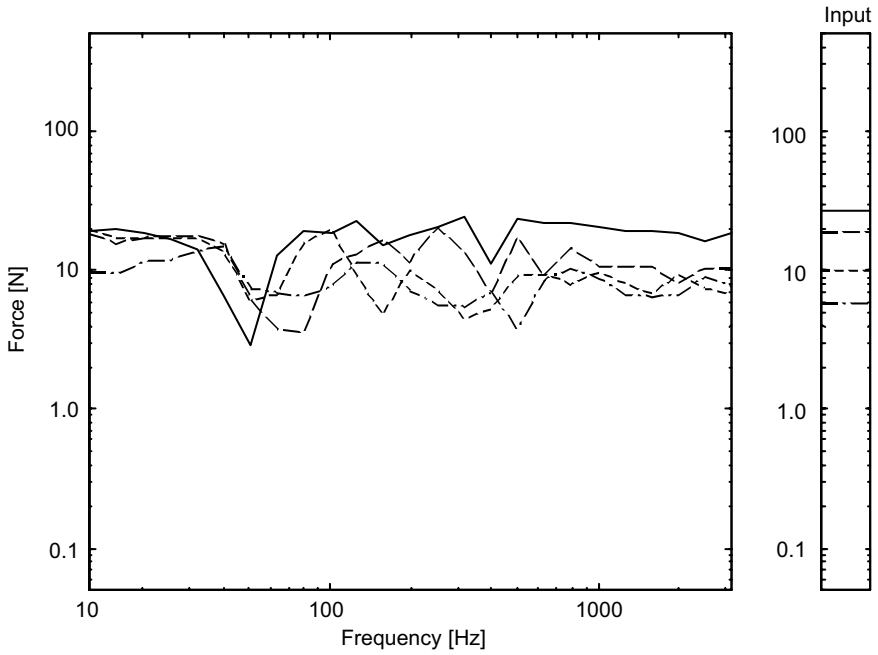

Fig. 7. Reconstructed forces in one-third octave bands for four sources and four responses. Singular values rejected based on the error band of ± 3 S.D. in accelerance estimation. ——— , force 1; — — — , force 2; – – – – , force 3; — · — · — , force 4.

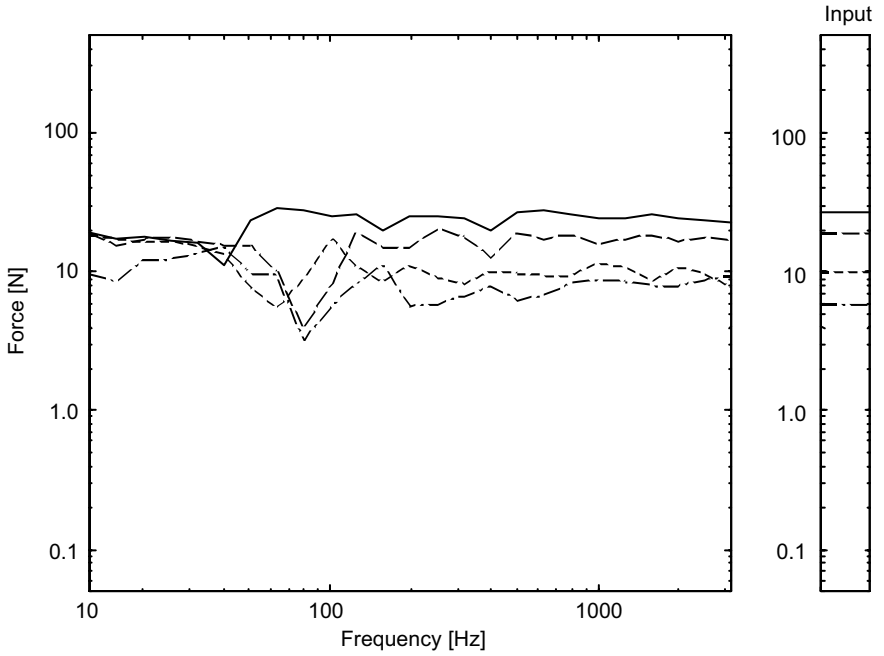

Fig. 8. Reconstructed forces in one-third octave bands for four sources and four responses. Singular values rejected based on the error band of ± 1 S.D. deviation in accelerance estimation. ——— , force 1; — — — , force 2; – – – – , force 3; — · — · — , force 4.

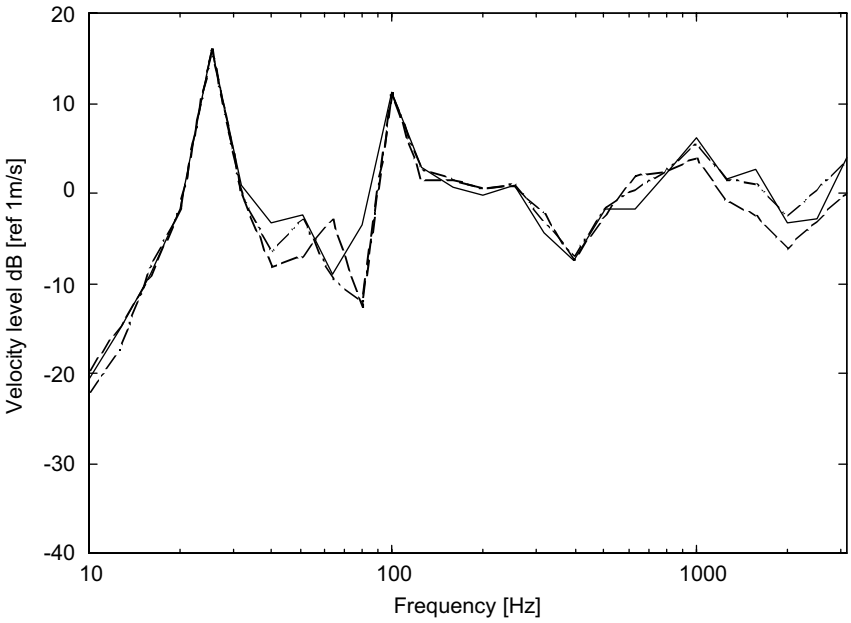

Fig. 9. One-third octave band velocity response for four sources and four responses with singular value rejection based on error estimates in accelerance. — — — , Predicted response by ± 3 S.D.; — · — · — , predicted response by ± 1 S.D.; ——— , actual response.

condition numbers are moderately high and the error in the accelerance measurement is large, it is important that these singular values are not ignored, as the threshold criterion described earlier can discard some useful information in this situation. Hence to generalize, the cumulative sum of the last $(n-r)$ singular values should be compared while discarding the singular values. Fig. 10 shows two of the reconstructed forces obtained by these two strategies. In the low-frequency region using the cumulative sum of singular values for comparing with the threshold is found to give a slightly better estimation. Further results are given in Ref. [12].

3.2.2. *Threshold based on response error*

In the above, it is assumed that the main source of error is the FRF matrix. However, the operational responses also form a source of error, and since they are often measured in a noisier environment, this may be dominant. The second criterion explored for threshold estimation for the singular values is, therefore, based on the contribution of individual singular values to the operational response. This has been proposed recently in Ref. [7] but is not widely used. The operational responses can be written as a summation of contributions from each of the singular values. According to this criterion, smaller singular values are rejected if they contribute less than the estimated error in the measurement of operational responses. The errors in the operational responses can be estimated based on a covariance matrix recorded during the measurements [4] or by using the relations as in Ref. [9]. If estimated from the latter, the random error in the operational response measurements can be based on the expression for the standard deviation for a Gaussian signal.

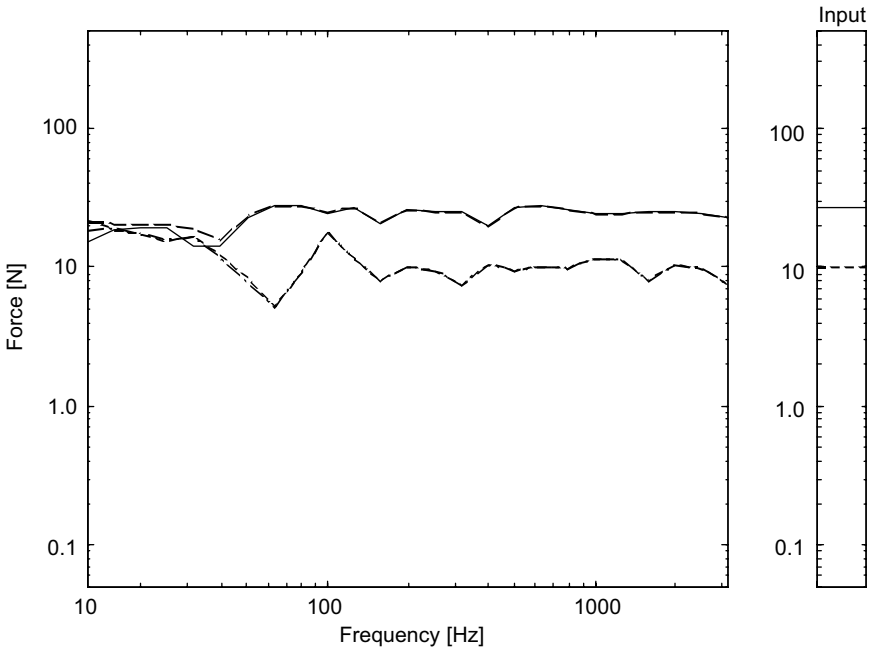

Fig. 10. Example of reconstructed forces in one-third octave bands for four sources and four responses by singular value rejection based on the error band of ± 1 S.D. in accelerance estimation. ——— , force 1; – – – – , force 3: comparison by individual singular values; — — — , force 1; — · — · — , force 3: comparison by cumulative sum of singular values.

$$\sigma^2 = \frac{(\hat{\mathbf{S}}_{xx})^2}{\sqrt{n_s}}, \tag{5}$$

where n_s is the number of samples taken for averaging and S_{xx} is the PSD of x. Based on [7] the singular value s_i should be rejected when

$$s_i \leqslant \frac{||\{\sigma\}||_2}{||\{\hat{\mathbf{a}}\}||_2} s_1. \tag{6}$$

In the present case, the forces identified by this technique are found to be similar to those obtained using the threshold based on E_{ij} [12]. Hence the responses predicted are also similar.

Further improvements are observed in the force identification in this case as well, if instead of comparing individual singular values, the cumulative sum of the last $(n-r)$ singular values is compared with the threshold [12]. In general, for both types of threshold, it can be concluded that while comparing singular values, the cumulative effect of singular values rejected earlier should be considered.

3.2.3. Failure of existing threshold criterion

There are some limitations in both types of threshold described above. The errors in the FRFs and responses need not happen simultaneously. These could be dominant at different frequencies. Hence using a threshold based on one error or the other might not be sufficient. Although the

errors in the FRFs are expected to be smaller than the errors in the responses, since the former are measured in a controlled environment, at antiresonance the reverse may be true. This is confirmed by Fig. 11. The upper plot shows a situation where singular value rejection based on the FRF errors fails. Here the FRF error is smaller (reduced to 5% of the original FRF error) than the response errors. Hence, the technique with a response error based threshold succeeds in improving the prediction. On the other hand, the response error based technique is less successful when FRF errors are dominant, as shown in the lower plot where the response error is reduced to 2.5% of the original noise level. This illustrates that these techniques on their own cannot be applied universally. Further work is needed to develop a threshold based on a combination of FRF errors and response errors. In the following sections an alternative technique is introduced which can have this effect.

3.3. Resampling of accelerance

It has been seen that errors in the FRF matrix $\hat{\mathbf{A}}$ lead to errors in the forces. However, supposing the errors in the measured FRFs are small and random, for a given measurement $\hat{\mathbf{A}}$, the actual accelerance lies within a confidence interval around $\hat{\mathbf{A}}$ as shown in Fig. 12. Suppose that a new set of measurements is made for the accelerances for each sample $\hat{a}$ used to estimate the forces $\hat{\mathbf{F}}$. This would allow the effect of random errors in $\hat{\mathbf{A}}$ to be averaged out and improve the mean of the identified forces, provided a large number of samples are taken. This technique, resampling of

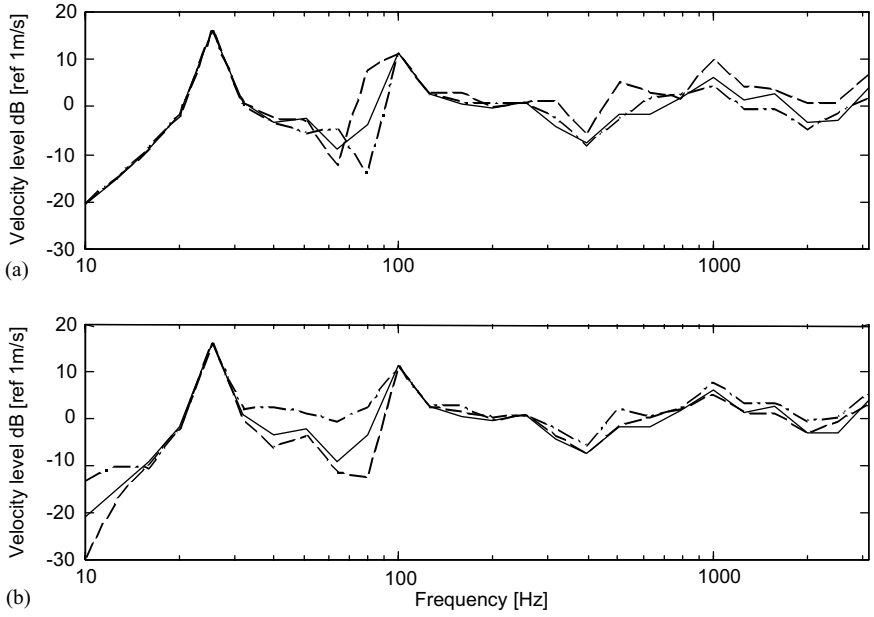

Fig. 11. One-third octave band velocity response for four sources and four responses with singular value rejection—example of a simulation where this technique fails: (a) failure of FRF error based technique—response errors are significantly larger than FRF errors; (b) failure of response error based technique—FRF errors are significantly larger than response errors. — — — , based on error in accelerance; — · — · — , based on response error; ——— , actual response.

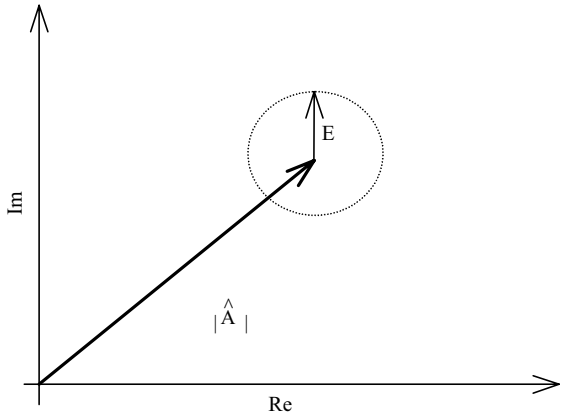

Fig. 12. Phasor representation of accelerance along with the error.

the accelerance matrix, has been implemented in simulations and the results were encouraging [10]. To put it into practice, however, could be difficult since the number of measurements required is enormous.

Nevertheless, it is possible to simulate the effect by perturbing the measured accelerance matrix $\hat{\mathbf{A}}$ with random noise before pseudo-inversion. The magnitude of the perturbation is based on the coherence at the frequency of calculation, along with the magnitude of the accelerance at that frequency. The expression for the standard deviation of the FRF error, given by Eq. (4) with $\alpha = 1$, can be used for this purpose. The expression for the modified accelerance matrix is

$$\hat{\mathbf{A}}_{\omega k} = \hat{\mathbf{A}}_{\omega} + \mathbf{A}_{pert}, \tag{7}$$

where $\mathbf{A}_{pert} = \mathbf{N}_{nd}\mathbf{E}e^{j2\pi N_{nu}}$ is a perturbation matrix, N_{nd} is a random number with variance 1 and zero mean (normally distributed) and N_{nu} is a random number between 0 and 1 (uniformly distributed). This error can be represented in the phasor diagram shown in Fig. 12. The zone within the circle indicates schematically the possible values that the accelerance can take. Since the estimated accelerance is expected to be biased, the actual envelope will differ slightly from that shown. The perturbation will only take care of random errors, which is acceptable since bias errors do not magnify significantly [13].

Fig. 13 shows the predicted response in one-third octave form from the perturbation technique. Significant improvements are seen compared with the ordinary inverse method. From further investigation, however, this method has been observed to be very sensitive to the amplitude of the error of the operational responses, that is it only works well when the errors in the operational responses are small compared with those in the FRFs.

3.4. Rejection of perturbed singular values

In Section 3.2, where singular value rejection has been studied, it was observed that the thresholds for the rejection of singular values based on accelerance error or response error are not universally applicable. The success of these two thresholds depends on the respective noise levels

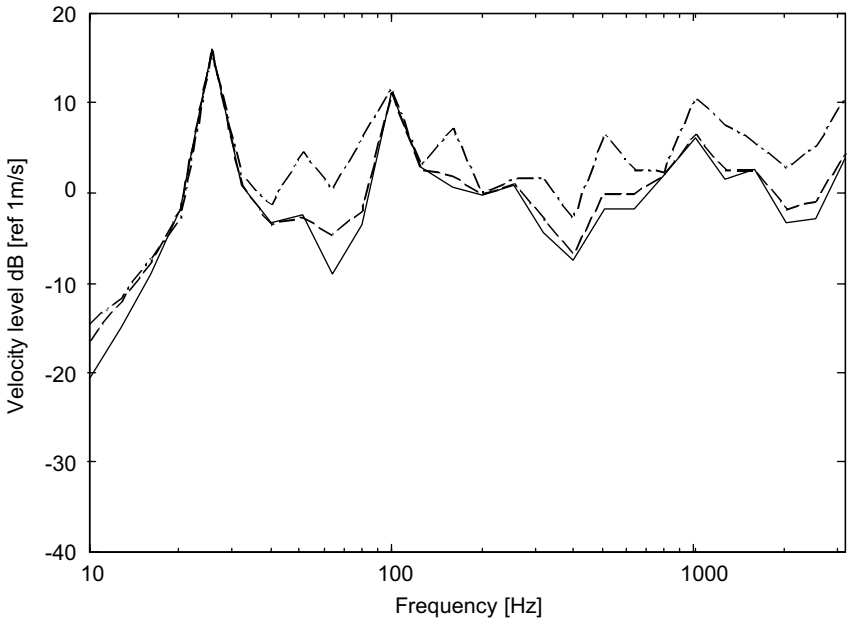

Fig. 13. One-third octave band velocity response for four sources and four responses with perturbation of accelerance matrix. — — — , predicted response by perturbation; — — · — , predicted response without perturbation; ——— , actual response.

in the accelerances and responses. It is desirable to develop a technique which can take care of both kinds of errors, whatever their level. The perturbation technique can be exploited to provide a solution.

It is helpful to compare the error reduction achieved by the perturbation technique and the threshold based on accelerance errors. Their results differ slightly as no information is lost in the perturbation technique so the results will be less biased than those from singular value rejection, provided the response error is small. The latter restriction ensures that the amplification of response errors does not occur. This can be overcome by additionally rejecting singular values based on the response error norm. The net effect would then be to perturb the accelerance matrix and reject perturbed singular values if they are smaller than the response error norm.

This combination allows the error magnification due to FRF errors to be reduced by perturbation, while singular value rejection minimizes the error magnification due to response errors. In the presence of large response errors, singular value rejection based on them will reduce the error amplification. In this case the perturbation will tend not to have much effect since perturbation mainly affects the smaller singular values which are already rejected. On the other hand if the response error is smaller than the FRF error, singular values will not be rejected and since perturbation of the accelerance matrix works robustly for small response errors the results will still be reliable. Hence, a method has been established which should produce reliable results whatever the error level in responses or FRFs.

Numerical simulations have been carried out that confirm the superiority of this method. Fig. 14 shows the responses predicted for various levels of errors in FRFs and responses. The method suggested is found to be robust for all combinations of errors considered. Three cases of

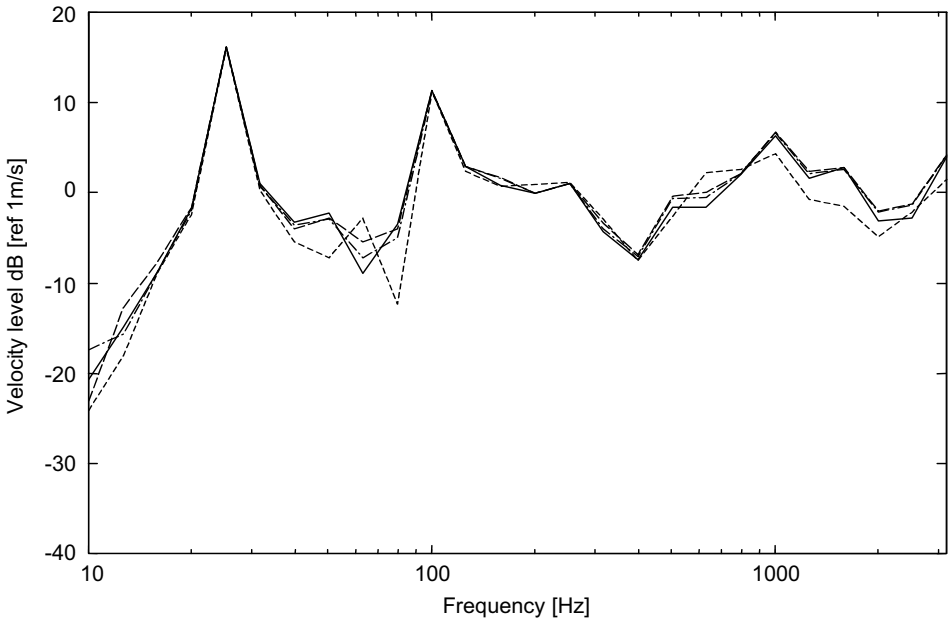

Fig. 14. One-third octave band velocity response for four sources and four responses with singular values rejected based on the error band of ± 1 S.D. in response error and with perturbation of accelerance matrix. — — — , large FRF error and small response error (failed case of Fig. 11); – – – – , large FRF error and large response error; — · — · — , large FRF error and moderate response error; ——— , actual response.

error combinations were considered in the simulation. In the first case the FRF error is dominant compared to the response error (2.5% of the original noise in the response). In this combination, the result by singular value rejection based on the response error is less successful as seen from Fig. 11b. Comparison of Figs. 11b and 14 shows significant improvement when singular value rejection is combined with the perturbation technique for the same case. The case where both FRF and response errors are large is the same as those shown in Figs. 6 and 9. No improvement is observed in this situation by combined singular value rejection and perturbation technique compared to singular value rejection alone since most of the small singular values are rejected due to the large threshold value. However, the method still results in a consistent prediction. In the last case the FRF error is dominant again (response error is 25% of the original noise level) and predictions are reasonably good.

4. Experimental validation

4.1. Experiments

In order to validate the various concepts considered above, experiments have also been carried out. The experimental set-up consists of a flat rectangular plate ($700 \times 500 \times 1.5\,\text{mm}^3$) made of steel, hung from a frame using elastic threads. Two electrodynamic shakers were used for excitations representing the operational response. These were fed with signals from the same

signal generator and the amplitudes of the forces were varied independently by adjusting the gain on the amplifier. The shakers were connected to the plate through force gauges. The force gauges were mounted on the plate in such a way that the mass loading was minimal. Accelerometers and force gauges were mounted on cementing studs, which were glued to the plate. This was done to ensure repeatability, particularly in the high-frequency range, by eliminating any spatial deviations. Additional damping was introduced by damping films glued to the back of the plate.

A frequency range of 30–1600 Hz was used in the analysis. Below 30 Hz the coherence was found to be very low and errors were large in FRF estimates. The frequency resolution was 1 Hz. Coherence improvement because of further refinement of the resolution was found to be small.

The measurements performed consisted of operational responses measured at a series of locations on the plate when both shakers were in operation (this represents a situation where some machine is mounted on the plate), and FRFs from each of three forcing locations to the various response locations. These were measured keeping one shaker operational and disconnecting the other shaker. All transducers were left screwed to the plate through cementing studs during these measurements. One of the forces is included in the experiment but actually had zero amplitude in the operational response measurements. This is to ensure that the problem is of sufficient size to provide realistic matrix condition numbers whilst remaining a practical measurement.

4.2. Experimental force identification

All data were captured initially as time histories. The amplitude of the operational response is taken as the square root of the auto spectrum and the phase is given by that of the cross-spectrum between the response and a reference signal. One of the responses is taken as the reference signal. The expression for the response can thus be written as

$$a_i = \sqrt{G_{ii}} e^{i \angle G_{i,k}}, \tag{8}$$

where i is a response number and k is the reference response number.

One of the operational forces was deliberately always larger than the other one by an average of 3.5 dB. The coherence between these two forces was checked and it was concluded that they were coherent [13] (in most of the frequency range considered $\gamma^2 > 0.9$).

One of the frequency responses (accelerance) is given in Fig. 15. From this figure, the first few modes can be seen to have quite high damping. The coherence is poor at low frequencies and at 50, 150, and 250 Hz due to mains interference. Modal damping ratios have been obtained from the measured FRFs using the half power bandwidth for the first few modes. These were found to decrease from 0.08 at 30 Hz to around 0.01 at 100 Hz.

The forces identified by Moore–Penrose pseudo-inversion contained large errors, particularly the smaller force [14]. Errors were observed to be large at some high frequencies even though the condition numbers were not so high in this region. Fig. 16 shows the velocity predicted at one of the locations on the plate, which also follows the same trend. These results are plotted in bands of constant (15 Hz) bandwidth. The consistent under-prediction may be related to the assumption that forces are coherent, when in practice the coherence was between 0.9 and 1. Use of singular value rejection based on the threshold determined from FRF errors did not result in improvements to the forces identified. This could be due to the amplitude of the errors in the

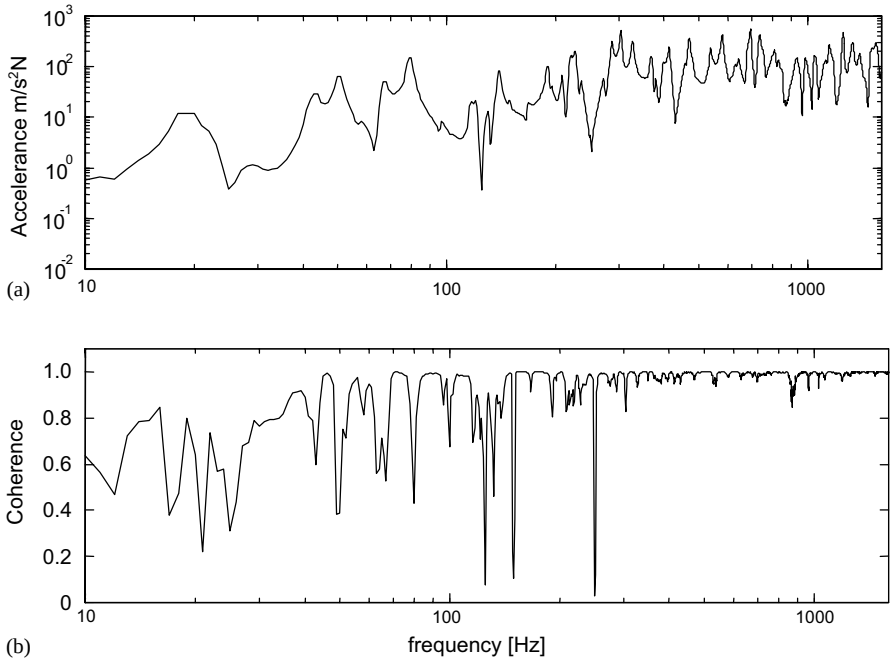

Fig. 15. Typical experimental FRF: (a) accelerance magnitude and (b) coherence.

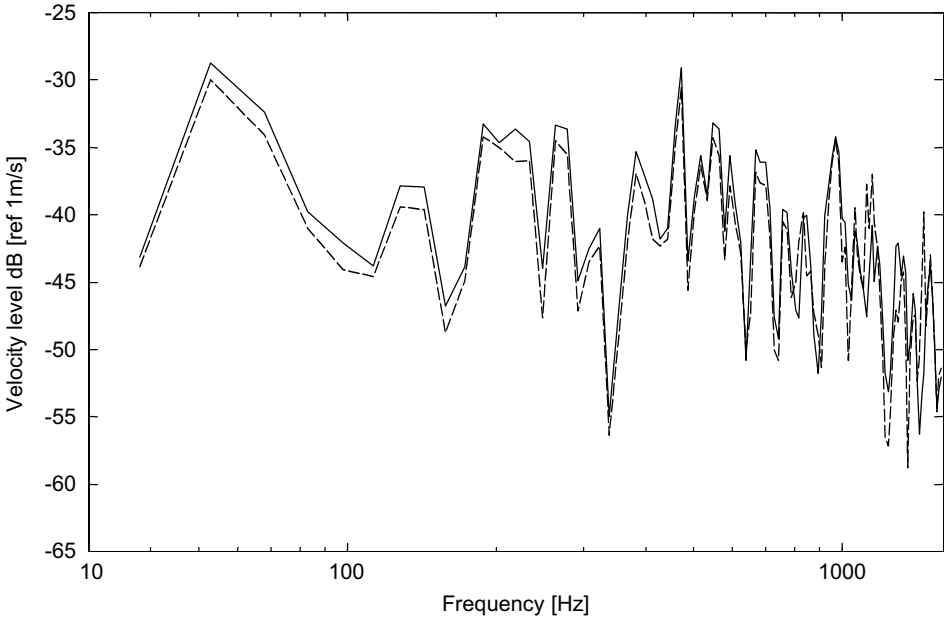

Fig. 16. Predicted response by pseudo inverse method from experimental results for three forces and four responses. — — — , predicted response; ——— , actual response.

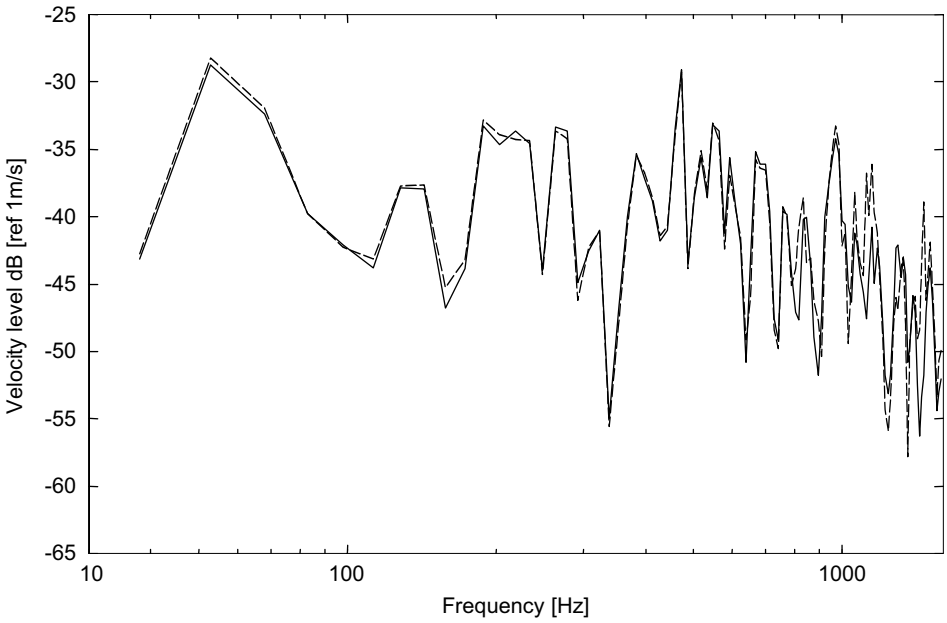

Fig. 17. Predicted response by perturbation technique from experimental results for three forces and four responses. — — — , predicted response; ——— , actual response.

FRFs being smaller than the operational response errors. The velocity predicted using this method did not differ from that given by the Moore–Penrose pseudo-inverse.

There was a significant improvement in the high-frequency region in the force identification when using singular value rejection based on the threshold from operational response errors. However, the forces were underestimated in the low-frequency region [14]. The reason for the improvement at high frequencies is due to the presence of higher response errors in that region. Similarly, the velocity predicted by this method was accurate in the high-frequency region but underestimated in the low-frequency region.

The FRF resampling technique results in extremely good force identification in the low-frequency region. However, errors continue to occur at high frequencies. The velocity predicted by this method is shown in Fig. 17, which confirms the significant improvement in the low-frequency region. The resampling technique in combination with singular value rejection does not result in significant improvements over singular value rejection alone in this case because most of the small singular values are rejected due to the large threshold.

5. Conclusions

Using both simulations on a simply supported rectangular flat steel plate and measurements on a hanging rectangular flat plate, it has been shown that the determination of forces by inverse methods can be improved by various techniques. Although over-determination does not yield much improvement in force estimates at low frequencies, it improves response estimates

considerably. At higher frequencies, where the modal overlap is greater, over-determination gives significant reduction in condition numbers and hence improvement in forces and responses.

Singular value rejection can be a powerful tool for reducing error magnification. Threshold criteria based on estimates of error in either FRFs or operational responses have been explored, but neither is universally applicable. Ideally a criterion based on both forms of errors is required.

A means of achieving this has been proposed based on FRF resampling using a perturbation technique. This was found to be effective where FRF errors were dominant, but in simulations where the response error was larger it was less effective. However, by combining it with singular value rejection based on errors in operational responses, the combined technique works effectively as a threshold criterion based on both FRF and response errors.

For simplicity the work has been based on a rectangular plate. Built-up structures could pose different complexities due to the multi-axial nature of the problem. This may result in difficulties in choosing the number and direction of forces. Built-up structures also result in interaction between different waves, which cannot be considered in the case of the plate studied. Nevertheless, the techniques which are studied here do not depend on the details of the structure and should perform equally well for any structure, provided the choice of force and response positions is sufficient to represent the wave fields present in the structure.

In a companion paper some alternative regularization techniques are considered to overcome problems of matrix ill conditioning [15].

References

[1] P. Mas, P. Sas, K. Wyckaert, W. Hendrickx, P. Van Der Linden, Noise and vibration transfer path analysis, Proceedings International Seminar on Applied Acoustics ISAAC 6, Vol. IV, Leuven, 1995, pp. 1–22.

[2] U. Fingberg, T, Ahlersmeyer, Noise path analysis of structure-borne engine excitation to interior noise of a vehicle, Proceedings of the 17th International Seminar on Modal Analysis, Leuven, Belgium, 1992, pp. 143–152.

[3] J. Romano, J.A. Lopez, Practical application of transfer path analysis to resolve structure-borne noise problems in vehicle design, Proceedings of the 21st International Seminar on Modal Analysis, Leuven, Belgium, 1996, pp. 527–536.

[4] M.H.A. Janssens, J.W. Verheij, D.J. Thompson, The use of an equivalent forces method for the experimental quantification of structural sound transmission, Journal of Sound and Vibration 226 (1999) 305–328.

[5] J.W. Verheij, Inverse and reciprocity methods for machinery noise source characterization and sound path quantification, Part 1: sources, International Journal of Acoustics and Vibration 2 (1) (1997) 11–20.

[6] J.W. Verheij, Inverse and reciprocity methods for machinery noise source characterization and sound path quantification, Part 2: transmission paths, International Journal of Acoustics and Vibration 2 (3) (1997) 103–112.

[7] M.H.A. Janssens, J.W. Verheij, T. Loyau, Experimental example of the pseudo-forces method used in characterisation of a structure-borne sound source, Applied Acoustics 63 (1) (2002) 9–34.

[8] G.B. Warburton, The Dynamical Behaviour of Structures, 2nd Edition, Pergamon, Oxford, 1976.

[9] J.L. Bendat, A.G. Piersol, Engineering Application of Correlation and Spectral Analysis, 2nd Edition, Wiley Interscience, New York, 1993.

[10] A.N. Thite, D.J. Thompson, Study of indirect force determination and transfer path analysis using numerical simulations for a flat plate, ISVR Technical Memorandum No. 851, May 2000.

[11] J.A. Fabunmi, Effects of structural modes on vibratory force determination by pseudo-inverse technique, American Institute of Aeronautics and Astronautics Journal 24 (3) (1986) 504–509.

[12] A.N. Thite, D.J. Thompson, Further study of indirect force determination and transfer path analysis using numerical simulations for a flat plate, ISVR Technical Memorandum No. 854, October 2000.

[13] M. Blau, Indirect measurement of multiple excitation spectra by FRF matrix inversion: influence of errors in statistical estimates of FRFs and response, Acustica 85 (1999) 464–479.
[14] A.N. Thite, D.J. Thompson, Experimental validation of force identification techniques, ISVR Technical Memorandum No. 862, May 2000.
[15] A.N. Thite, D.J. Thompson, The quantification of structure-borne transmission paths by inverse methods. Part 2: Use of regularization techniques, Journal of Sound and Vibration 264 (2003) 433–451, this issue.